Time Dependent Analysis of Tunnels Using The Finite Element Method

Dr. Mohammed Y. Fattah Dr. Kais T. Shlash* & Dr. Nahla M. Salim*

Received on: 2/3/2008
Accepted on:7/8/2008

Abstract

The analyses of tunnels in clay were carried out taking into consideration two great important and effective categories, the time independent and time dependent. Time independent behaviours are used to represent the excavation stage while time dependent analyses are used to represent the behaviour of the unlined tunnel after a long time.

The finite element analyses were carried out using the linear elastic model for the concrete liner while elasto-plastic and modified Cam clay model for the soil. The excavation has been used together with transient effects through a fully coupled Biot formulation. All these models and the excavation technique together with Biot consolidation are implemented into finite element computer program named "Modf-CRISP" developed for the purpose of these analyses.

In this paper, the basic problem represents the proposed "Baghdad metro line" which consists of two routes of (32 km) long and 36 stations is analyzed. The tunnel is circular in cross section with a (5.9) m outer diameter and (0.45) m of concrete lining thickness. Eight-node isoparametric elements are used to model the soil and concrete lining. Four-node element is used for pore water pressure.

Two kinds of analyses are carried out:

a- Using elastic-plastic constitutive model for all soil layers.

b- Using modified Cam clay model (MCC) for the first soil layer (upper layer) and elastic-plastic Mohr Coulomb for the other two layers.

The movements of the soil around the tunnel at the end of excavation at typical points (crown, spring line and the invert) are calculated. The results indicate that there is an inward movement at the crown and this movement is restricted to four and a half tunnel diameters. A limited movement can be noticed at spring line which reaches 0.05% of tunnel diameter, while there is a heave at the region below the invert, which reaches its maximum value of about 0.14% of the diameter and is also restricted to a region extending to (1.5) diameters.

It was found that the maximum consolidation settlement above the tunnel is about three times that at the end of excavation. The settlement trough extends only to (5) tunnel diameters using consolidation analysis while it is extended to (12) tunnel diameters using undrained analysis.

التحليل المعتمد على الزمن للانفاق باستعمال طريقة العناصر المحدودة

الخلاصة

إن تحليل الأنفاق في الترب الطينية تم إجراؤه مع الأخذ بنظر الاعتبار ظاهرتين فعاليتين ومهمتين وهما الاعتماد وعدم الاعتماد على الزمن. يستعمل التصرف غير المعتمد على الزمن لتنفيذ مرحلة الحفريات بينما يستعمل التصرف المعتمد على الزمن لتمثيل تصرف النفق غير المبطن عبر فترة طويلة من الزمن.

أجري تحليل العناصر المحددة باستعمال نموذج خطي مرن لمادة كونكريت التبطين بينما أستعمل النموذج المرن اللدن ونموذج طين كام لتمثيل التربة. اخذ تأثير كل من الحفريات وتاثير الزمن معا من خلال التمثيل المزدوج الكامل بالاعتماد على نظرية بيوت (Biot). إن هذه النماذج والتمثيلات مع طريقة الانضمام تم تضمينها في برنامج حاسبة للتحليل بطريقة العناصر المحددة يسمى "MODF-CRSP" والذي تم تطويره لهذا الغرض.

* Building and Construction Engineering Department, University of Technology/ Baghdad

https://doi.org/10.30684/etj.27.1.10
2412-0758/University of Technology-Iraq, Baghdad, Iraq

في هذا البحث تم تمثيل المسالة الرئيسية بمقترح مترو بغداد الذي يتألف من خطين بطول 32 كم و36 محطـــة. مقطع النفق دائري بقطر (5.9 م) مع وجود تبطين خرساني بسمك (0.45 م) واستعملت عناصر ثمانيـــة العقـــد لتمثيل التربة وللبطانة الخرسانية بينما استعملت عناصر رباعية العقد لتمثل ضغط الماء المسامي.
اجري نوعان من التحليل:
أ- استعمال علاقة تكوينية مرنة لدنة لتمثيل جميع طبقات التربة.
ب- استعمال نموذج كام المعدل لتمثيل طبقة التربة العليا ونموذج مور -كولوم المرن اللدن لبقية الطبقات.
ولقد تم حساب إزاحات التربة حول النفق في نقاط محددة (القمة , جوانب وقعر النفق) في نهاية فترة الحفر.
وقد بينت النتائج أن هناك حركة للداخل عند قمة النفق وتكون هذه الحركة محددة 5و4 مرة بقدر قطـــر النفـــق بينما وجد أن الإزاحة محدودة عند جوانب النفق ويمكن أن تصل 0.05 من قطر النفق كمـــا ووجـــد أن هنـــاك انتفاخا في المنطقة الواقعة تحت قعر النفق والتي تصل قيمتها القصوى بحدود 0.14 % من قطر النفـــق وهـــي محددة بمسافة تمتد إلى 1.5 مرة من قطر النفق.
وقد وجد أيضا أن هبوط الانضمام فوق النفق يكون بحدود 3 مرات الهبوط عند نهاية الحفـــر ويمتـــد حـــوض الهبوط إلى مسافة بحدود 5 مرات قطر النفق عند اعتماد تحليل الانضمام بينما يمتد هذا الحوض إلـــى 12 مـــرة بقدر قطر النفق عند الاعتماد على التحليل غير المبزول.

Introduction

The growth of many cities has resulted in the need for increased infrastructure. As an urban space becomes more limited, subsurface structures such as tunnels are becoming more efficient in providing the required infrastructure. In 1863, the first underground railway line was opened in London. Since then over 100 cities worldwide have implemented underground transport systems and over 50% of them are undergoing development or expansion (*Hellawell et al., 2001*).

Some Aspect of Soil Behavior around Tunnels

Time-independent Effects:

The effect of tunneling on the displacements and stresses around underground tunnel openings and on the surface displacements due to excavation of these openings rely on time-independent effects.

The relative magnitude of short and long term movements depends on many factors. *Simons and Som, (1970),* and *Morton and Au, (1975),* suggested that for typical site on stiff clay, about 60% of the total settlement occurs in the short term while *Attewell and Selby, (1989),* observed that long term settlements up to 2.5 times the short term, and also the long term trough widths tended to be wider.

Giod and De Doneto, (1979), used a linear elastic plastic model with Mohr-Coulomb failure surface for the soil. The tunnel lining is simulated using thin elements whose properties are changed during the analysis. This models the imposition of a sprayed concrete lining which subsequently gains strength and stiffness over time. The surface settlement profiles predicted by this model are wider than expected in practice.

Ezzeldine, (1999), used the finite element analysis to study the expected ground movement due to the tunnel construction and compare it with ground control measures imposed during the construction process. The analysis was carried out at the part of line from Khalafawy to Saint- Therese station. The study is based on an available documentation related to the ground construction to emulate the most probable model to be adopted. A nonlinear stress–strain constitutive model is adopted to represent the ground surrounding the tunnel. The results are predicted in terms of the maximum displacement at the ground

* Building and Construction Engineering Department, University of Technology/ Baghdad

surface and the slope of the displacement trough. It was shown that, the settlement trough extends to about 5 diameters from the tunnel centerline and also, the maximum slope of displacement varies between (1/1500) to (1/500) and the maximum point of maximum slope takes place at about one of the diameter from the tunnel centerline.

Time-dependent Effects

Time dependent effects play an important role in the design and construction of tunnels. The failure of excavated tunnels often occurs immediately or during several decades after excavation. The reason for this instability can be attributed to the following:

- The dissipation of pore water pressure.
- The deterioration of materials.
- Progressive failure.

In general, when a tunnel is excavated in fully saturated soil, two types of time dependent behaviours occur in the surrounding ground. The first comes from the intrinsic rate dependent characteristic of the material such as creep deformation or stress relaxation and the second is caused by the loss of apparent strength of material due to dissipation of the excessive pore water pressure in the surrounding ground. So the time dependent behaviour can be modelled using a coupled Biot consolidation finite element approach.

Definition of the Basic Problem

In the present study, the basic problem represents "Baghdad metro line" which consists of two routes of (32 km) long and 36 stations. The tunnel is circular in cross section with a (5.9) m outer diameter and (0.45) m of concrete lining thickness. The geological section for a specified position with tunnel axis at a depth of (18) m is shown in Figure (1).

Boundary Conditions of Numerical Analysis and Material Parameters

The material parameters used in the analysis of Baghdad metro are given in Table (1). Figure (2) shows the finite element mesh used in the numerical analyses and the following supposed conditions are used:

1. The boundary condition is that there is only horizontal restriction on the left and right vertical sides, and there are both horizontal and vertical restrictions at the bottom boundary.
2. The problem boundaries are assumed to be impermeable on both vertical sides in addition to the bottom boundary. The water table is at the ground surface.

Eight-node isoparametric elements are used to model the soil and concrete lining. Four-node elements are used for modelling pore water pressure. Symmetry is assumed along the tunnel vertical axis containing the crown, spring line and invert. This situation makes it possible to mesh just one half of the entire geometry as shown in Figure (2). The excavation process is assumed to occur under plane strain conditions since that the effect of advancing the tunnel at the face is not considered in this analysis. In linear elastic analysis, the excavation process can be applied in a single instantaneous step. In non-linear stress-strain relationship, the program CRISP allows the effect of element removal to be spread over several increments in an "increment block". Element stiffnesses are always removed in the first increment of a block, but the associated loads are distributed over all the increments in the block. The excavation process was assumed to last for two hours per meter length and in nonlinear analysis, it was spread over fifty increments.

Points of Interest when Analyzing a Tunnel

Figure (1) shows the location of points to be focused upon in the analysis:

1) The tunnel crown is the topmost point of the tunnel section (point A).
2) The spring line refers to point located at the side wall of the tunnel (point B).
3) The invert refers to the bottom of the tunnel section (point C).
4) The shoulder is referred to by point (D).

Undrained Analyses

Two kinds of analyses are carried out:

a- Using elastic-plastic constitutive model for all soil layers.

b- Using modified Cam clay model (MCC) for the first soil layer (upper layer) and elastic-plastic Mohr Coulomb for the other two layers.

The silty clay parameters used with MCC soil model are presented in Table (2). The parameters are calculated depending on the data of (*NCCLR, 1986*).

***Surface Settlement Due to Tunneling*:**

The magnitude of movements generally depends on the soil type, ground water condition, construction method, tunnel dimensions and location. Ground movements around tunnels lead to surface subsidence. The magnitude and distribution of these settlements were studied extensively by previous researchers (*Schmidt, 1969, Clough and Shmidt, 1981, O'Reilly and New, 1982, Rankin, 1988, and Mair and Taylor, 1993)*.

***Surface Settlement Due to Tunneling*:**

The magnitude of movements generally depends on the soil type, ground water condition, construction method, tunnel dimensions and location. Ground movements around tunnels lead to surface subsidence. The magnitude and distribution of these settlements were studied extensively by previous researchers (*Schmidt, 1969, Clough and Shmidt, 1981, O'Reilly and New, 1982, Rankin, 1988, and Mair and Taylor, 1993)*.

Tunnel construction inevitably leads to displacements in the soil, and these may lead to damage to nearby structures. These ground movements are associated with two mechanisms:

a) Radial movements of the soil as a result of cutting during tunnel construction.
b) Ground movements associated with incomplete support of the tunnel face.

Figure (3) shows the variation of surface settlement due to tunneling using two different constitutive models; elastic-plastic and modified Cam clay (MCC) for the first layer. It can be seen that the maximum settlement using MCC for the first layer is 4.4 mm, while the maximum settlement using Mohr Coulomb for the first layer is 4.2 mm. This is due to lower value of plastic stiffness of the soil given by the MCC model which produces larger plastic strains. The settlement that is caused by the accumulation of the vertical displacement of all the elements above the tunnel is also greater in the case of the MCC model. From the results, it can be seen that the constitutive models of the first layer have small effect on the settlement above the crown.

Figure (4) shows that the dimensionless settlement above the crown using Mohr Coulomb is about 0.17% greater than the dimensionless settlement using MCC constitutive model. It is also shown that, most deformations occur near the tunnel opening and they are largely restricted to a zone within twice tunnel diameters.

It can also be concluded from Figures (3) and (4) that the two constitutive relations; Mohr-Coulomb and MCC give approximately similar

displacements when the distance from center of the tunnel increases.

Figure (5) shows the variation of vertical movement at different points around the tunnel during excavation (which was assumed to last 2-hours). In this figure, negative movement means an inward movement towards the tunnel's center while a positive value of vertical movement means and upward movement towards the tunnel center. There is an inward movement at the crown and all points above the center of the tunnel, while there is an upward movement at the invert and all points below the center line of the tunnel. This means that there is a heave taking place at all points below the center line of the tunnel. At the spring line, very small movement of about 0.05% of the diameter occurs, while the inward movement may reach 0.15% of the diameter at the crown and a maximum outward movement reaches 0.1% of the diameter at the invert. This difference is due to relatively high in situ stresses at the invert and low soil strength and usually the invert is not allowed to have perfect arch for stress redistribution (*Weishen et al., 2003*).

The same results are obtained in Figure (6) using MCC constitutive model, except that the maximum settlement at the crown reaches approximately 0.175% of the tunnel diameter.

Movement of the Soil around the Tunnel

The movements of the soil around the tunnel at the end of excavation at typical points (crown, spring line and the invert) are shown in Figure (7). The results indicate that there is an inward movement at the crown and this movement is restricted to four and a half tunnel diameters. A limited movement can be noticed at the spring line which reaches 0.05% of tunnel diameter, while there is a heave at the region below the invert, which reaches its maximum value of about 0.14% of the diameter and is also restricted to a region extending to (1.5) diameters.

Figure (8) indicates the dimensionless settlement along section D-D; the radial distance above the crown, using two soil constitutive models. The results show that the maximum settlement reaches about 0.49% of the diameter near the center of the tunnel and is reduced to 0.08 % of the diameter at the surface using Mohr Coulomb soil model, while it reaches 0.7% of the tunnel diameter near the center of the tunnel and is reduced to 0.08% at the surface using MCC soil model.

Figures (9) and (10) represent the contours of vertical and horizontal movements, respectively. It is clearly shown that there is a downward movement at all points above the crown while there are upward movements (heave) for all points below the invert. Figure (11) shows the movement vectors which show the direction of movement of the soil surrounding the tunnel. It is clearly shown that all the points surrounding the tunnel move towards the center of the tunnel and it is restricted to a narrow region which is approximately less than D/2.

Stress Changes around the Tunnel:

Typical effective stress time history around the tunnel opening obtained by the finite element analysis is shown in Figure (12). The stresses are normalized by division of each stress by the initial overburden pressure. At the crown, excavation induces a reduction in the radial stress (σ_v') and a small increase in the tangential stress (σ_h') as shown in Figures (12a and 12b). However, the reduction of radial stress is rapid, this causes the radial stress to become the minor principal stress (σ_3) and the tangential stress to become the major

principal stress (σ_1). This means that the principal stresses rotate by 90^0 and s_1 remains horizontal after rotation. At the spring line, excavation induces a reduction in the radial stress (σ_h') to become (σ_3), and an increase in the tangential stress to become (σ_1). This means that the principal stresses do not change at the spring line as shown in Figure (12b). These results agree with the findings of *Lee and Rowe, (1989)*.

From this, the conclusion drawn is that the stress above and below the tunnel corresponds approximately to triaxial extension and that the strength and deformation profile in these regions can be estimated from triaxial extension tests, while near the spring line of the tunnel, the stress is intermediate between the triaxial compression and extension. This was also suggested by (*Lo and Rowe, 1982*), and (*Ng and Lo, 1985*). The modulus and strength parameters in this region should therefore lie between the compression and extension values. For this reason, the modulus above the crown and below the invert is most critical.

The variation of the horizontal and vertical effective stresses around the tunnel can be studied by plotting the relation between K which is (the ratio of initial horizontal to vertical effective stresses) and the excavation time which lasted two hours. Figure (13) shows that the value of K remains constant and starts with initial value of (1) because $\sigma_h' = \sigma_v'$ (normally stressed sand). This value starts to increase and reaches the maximum value over a period of time which is approximately 1.67 hrs.

Beyond this time, the value of K decreases dramatically at the crown which means that the horizontal stress increases and the vertical stress decreases due to tunneling. This is clear in Figure (13). The value of K at the crown reaches approximately 28; this is due to dramatic decrease in the vertical effective stress due to tunneling process, while at the spring line, the variation is very small. It is expected that the soil at the crown transforms gradually to overstressed sand due to excavation of the tunnel. This is confirmed by the results shown in Figures (14), (15) and (16) which show the absolute value of the overstress ratio (OSR= $\sigma_o'/\ \sigma_v'$) changes with time.

Figure (14) shows that at the crown, the OSR increases slowly at the start of excavation and then increases dramatically over a period of 1.67 hrs. This increase may be due to a great reduction in the vertical effective stress. Then the value of OSR is reduced sharply and reached about 5 at the end of excavation. The OSR at the invert follows the same trend as shown in Figure (15) but it tends to increase and reach approximately 25 at the end of excavation. Both cases indicate that the soil changes from normal stress to overstress due to great reduction in the effective vertical stresses caused by tunneling while at spring line the OSR is reduced as the process of excavation progresses (Figure 16).

The comparison between the OSR at the crown, spring line and the invert reveals that a great increase in the OSR occurs at the invert such that OSR at the invert is about 5 times that at the crown while there is a small reduction in OSR at the spring line due to continuous decrease in horizontal effective stress as a result of tunneling.

Figures (17) and (18) show the contour lines of vertical and horizontal effective stresses, respectively. It is clearly seen that the contour values of vertical effective stress increase with depth, but it is clear that the higher values concentrate near the tunnel wall. The contour values of horizontal effective stress also concentrate with

higher values above the crown and below the invert.

Consolidation Analyses

When a tunnel is excavated in a fully saturated soil, two types of time dependent behaviours occur in the surrounding ground. The first is due to the intrinsic rate dependent characteristics of the materials such as stress relaxation. The second is caused by movement of pore water due to the change of pore water pressure distribution in the surrounding ground. This section focuses on investigating the second type of time dependent behaviour of the surrounding ground.

The time dependent behaviour of tunnels can be modelled using a coupled consolidation finite element approach. In the following sections, the surface and subsurface settlements are studied using consolidation analyses for the first layer. The changes in excess pore water pressure are also considered.

***Surface Settlement*:**

Figure (19) shows the normalized surface subsidence at the end of excavation and after 10-year consolidation. The maximum settlement reaches approximately 0.2% of the tunnel's diameter when consolidation analysis is considered while the maximum value approximately equals 0.07% of the tunnel's diameter at the end of excavation. This means that the maximum consolidation settlement above the tunnel is about three times that at the end of construction. This increase in consolidation settlement is due to dissipation of excess pore water pressure that causes an increase in effective stresses which leads to increase in vertical movement. The results also show that the consolidation process causes the settlement trough to be deeper and narrower and the affected region is reduced. A small heave can be noticed at the far end which is at a distance about (5.75) of the tunnel diameter. This may be due to the flow direction of strain vectors which move inward to the tunnel for the elements near the tunnel and move upward for the ground surface at the farther side.

The settlement trough also extends to five (5) of the tunnel diameter using consolidation analysis while it is extended to twelve (12) of the tunnel diameter using undrained analysis. In general, the settlement predicted from consolidation analysis is about twice the settlement using short term at the end of excavation. This result agrees with the results of *Addenbrooke (1996)*.

Figure (20) shows the progress of surface settlement with time. The results show that, as the consolidation progresses, the settlement increases and the influenced region decreases. From Figure (20), the maximum consolidation settlement reaches approximately 0.2% of the tunnel diameter after 10 years while it reaches only 0.07% of the tunnel diameter at the end of excavation. In general, as the consolidation settlement progresses, the settlement trough gets deeper and narrower and the influenced region is reduced.

The progress of horizontal displacement with time is also studied. Figure (21) shows the horizontal displacement (normalized by the tunnel diameter) at different times. The results indicate that the maximum horizontal displacement occurs approximately at a distance of 2D at the end of excavation. This maximum horizontal displacement moves towards the tunnel opening as the consolidation progresses and it reaches its maximum value at a distance equal to 1.75D from the center of the tunnel after 10 years of consolidation.

Subsurface Settlement

In the previous section, the variation of the surface settlement with time due to consolidation is discussed. In this section, a subsurface settlement

is studied with time due to consolidation. The settlement is investigated at two sections; section B-B which is near the surface and about (5 m) from the ground surface and section C-C which is near the tunnel opening and approximately (13.5 m) from the ground surface. These two sections are shown clearly in Figure (2).

Figure (22) presents the variation of settlement along section (B-B) at different times. It can be seen that the subsurface settlement becomes deeper and the settlement trough width becomes narrower with time. The maximum settlement is approximately equal to (0.12%) of the tunnel diameter at the end of excavation and about (0.21%) of the tunnel diameter after 10 years of consolidation.

At section C-C, the effect of consolidation is not clear and the maximum settlement reaches (0.33%) of the tunnel diameter at the end of excavation and approximately (0.34%) of the tunnel diameter after 10 years of consolidation as shown in Figure (23). This is due to the fact that section C-C lies on the border between silty clay layer and silty sand layer at which the dissipation of excess pore water pressure takes place within very short time and during the excavation stage.

Horizontal Movement

The horizontal movement obtained from the finite element analysis (the negative sign refers to movement towards the tunnel) along the vertical line is shown in Figure (24) which profiles horizontal movement along section A-A at (5 m) offset from the tunnel center line. The maximum absolute horizontal movement is reached just above the tunnel axis at a depth of z = 18 m. The maximum movement towards the tunnel is approximately about (0.135%) of the tunnel diameter at the end of excavation then increases to (0.15%) of the tunnel diameter after ten years of consolidation.From there and away from the tunnel, the horizontal displacement is reduced and reaches its maximum value at about (8 m) from the surface then tends to move towards the tunnel centerline to reach its maximum value at the surface. It is about (0.045%) of the tunnel diameter at the end of the excavation and reaches its maximum value about (0.16%) of the tunnel diameter after consolidation.

Vertical Movement

Vertical displacement in terms of absolute values (the negative sign refers to movement towards the tunnel) reaches about (0.12%) of the tunnel diameter just above the tunnel axis of (z = 18m) as shown in Figure (25). This movement increases to approximately (0.15%) of the tunnel diameter at the end of 10 years of consolidation. The vertical displacement starts to increase above the tunnel axis towards the surface and reaches approximately (0.07%) of the tunnel diameter at the end of excavation and about (0.145%) of the tunnel diameter (-5 mm) after 10 years of consolidation. Below the tunnel center line, the vertical displacement tends to decrease dramatically and reaches its minimum value about (0.02%) of the tunnel diameter at a distance equals to (5 m) from the base of the mesh. The vertical movement tends to decrease as the consolidation process progresses and reaches very small value.

Conclusions

The modified Cam clay model revealed greater values of settlement in the soil than do the Mohr-Coulomb elastic-plastic model. This was attributed to the lower value of plastic stiffness of the soil assumed by the modified Cam clay model which produces larger plastic strains.

1. Most deformations due to tunneling in clays occur near the tunnel opening and they are restricted to a zone within twice tunnel diameters.
2. All points above the tunnel showed downward movement while those below the tunnel were subjected to upper movement due to tunneling.
3. At the crown of the tunnel, excavation induces a reduction in the radial stress (σ_v') and a small increase in the tangential stress (σ_h'). The reduction of radial stress is rapid which causes that this stress becomes the minor principal stress (σ_3) and the tangential stress becomes the major principal stress (σ_1). This means that the principal stresses rotate by 90^o after excavation and (σ_1) remains horizontal after rotation.
4. The maximum consolidation settlement above the tunnel is about three times that at the end of excavation. The settlement trough extends only to (5) tunnel diameters using consolidation analysis while it is extended to (12) tunnel diameters using undrained analysis.
5. In general, the settlement predicted from consolidation analysis is about twice the settlement using short term at the end of excavation

References

[1].Chapter 8, edited by E.W. Brand and R.P. Brenner, Elsevier.

[2].Ezzeldine, O.Y., (1999), "Estimation of the Surface Displacement Addenbrook, T.I., (1996), "Numerical Analysis of Tunneling in Stiff Clay", Ph.D. thesis, Imperial College, University of London.

[3].Al-Kinani, A. N., (2004), "Dynamic Analysis of R.C. Tunnels Subjected to Internal Explosions", Ph.D. Thesis, College of Engineering, University of Baghdad.

[4].Attwell, P.B. and Selby, A.R., (1989), "Tunneling in Compressible Soils", Large Ground Movements and Structural Implications", Tunneling and Underground Space Technology, Vol. 4.

[5]. Britto, A.M. and Gunn, M. J., (1987), "Critical State Soil Mechanics via Finite Elements, John Wiely and Sons, New York, U.S.A.

[6]. Clough, G.W. and Schmidt, B., (1981)." Excavation and Tunneling", in "Soft Clay Engineering", Field due to Construction of Cairo Metro Line Elkhalafawy-St. Therese", Tunneling and Underground Space Technology, Vol.14, No. 3, p.p. 267-279.

[7]. Franzius ,J.N.,(2003),"Behaviour of Building due to Tunnel Induced Subsidence", Ph.D. thesis, Imperial College, University of London.

[8]. Giod, G. and DeDonato, O., (1979), "Elastic-Plastic Analysis of Geotechnical Problems by Mathematical Programming", International Journal for Numerical and Analytical Methods in Geomechanics, Vol. 3, p.p. 381-401.

[9]. Hellawell, E. E., Hawley, A. J. , Pooley, S.D., Garrod, B. and Legett, M., (2001), "Metro Under Construction around the World", Proceedings Institution of Civil Engineers, Geotechnical Engineering, Vol. 149, p.p. 29-39.

[10]. Lee, K.M., and Rowe, R.K., (1989), "Deformation Caused by Surface Loading and Tunneling: the

Role of Elastic Anisotropy", Geotechnique Vol. 39, No.1, p.p.25-41.

[11]. Lo, K.Y. and Rowe, R.K., (1982), "Prediction of Ground Subsidence due to Tunneling in Clays", Research Report GEOT-10-82. London: University of Western Ontario, Canada.

[12]. Mair, R.J. and Taylor, R.N., (1993),"Prediction of Clay Behavior around Tunnels Using Elasticity Solutions", Proceeding Predictive Soil Mechanics Worth Memorial Symp., p.p. 449-463, Oxford.

[13]. Morton,K. and AU,E., (1975), "Settlement Observations on Eight Structures in London", Proceeding Conference ,Settlement of Structures, Cambridge , Pentech Press, p.p. 183-203.

[14]. NCCLR (1986), National Center of Construction Laboratories Research, Unpublished Report, Baghdad- Iraq.

[15]. Ng, R. M. C. and Lo, K. Y., (1985), "The Measurement of Soil Parameters Relevant to Tunneling in Clays", Canadian Geotechnical Journal , Vol. 22, No. 3, p.p. 375-391.

[16]. O'Reilly, M. P. and New, B. M. ,(1982), "Settlements above Tunnels in the UK-their Magnitude and Prediction", Tunneling, 82, p.p. 173-181.

[17]. Rankin, W., (1988), "Ground Movements Resulting from Urban Tunneling Prediction and Effects", Proceeding 23rd Conference of the Engineering Group of the Geological Society, London Geological Society, p.p. 79-92.

[18]. Schmidt, B., (1969), "Settlements and Ground Movements Associated with Tunneling in Soil , Ph.D. thesis. University of Illinois.

[19]. Simons, N.E. and Som, N.N., (1970),"Settlement of Structures on Clay with Particular Emphasis on London Clay", CIRIA Report 22.

[20]. Weishen, Z., Shucai Li, Shuchen Li, Weizhong, C., Lee, C.F., (2003), "Systematic Numerical Simulation of Rock Tunnel Stability Considering different rock Conditions and Construction Effects", Tunneling and Underground Space Technology , (18) p.p.pp.531-536

Table (1) The soil parameters of the analyzed section of the proposed Baghdad metro line (from Al-Kinani, 2004).

Type of soil	Modulus of Elasticity (E) (kPa)	Poisson's Ratio (ν)	Unit Weight (γ) (kN/m^3)	Permeability kx = ky (m/day)
Silty clay	80000	0.333	19.5	8.64×10^{-6}
Sandy to silty sand	180000	0.263	19.7	Drained
Sand	150000	0.284	20.0	Drained

Table (2) Cam clay parameters for Baghdad silty clay soil.

C_c	C_s	λ	κ	M
0.2	0.02	0.0866	0.00866	1.2

Note: $\phi = 30^o$.
where:

C_c: the compression index,
C_s: the swelling index,
λ : the slope of the normal consolidation line,
κ : the slope of the swelling line, and
M : gradient of the critical state line.

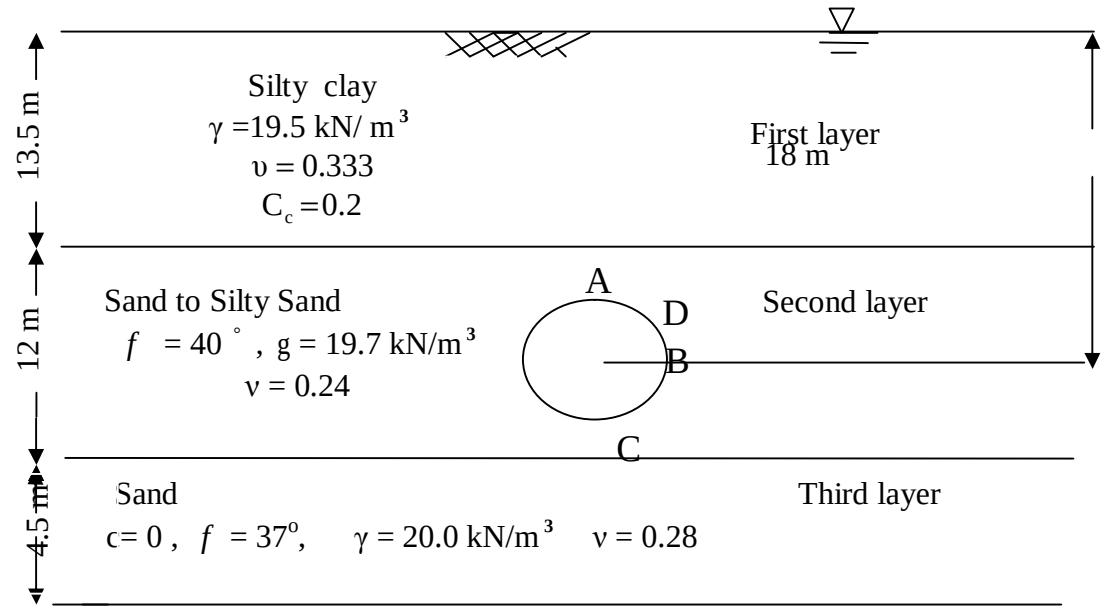

Figure (1) Geological profile and soil material properties along Baghdad metro line.

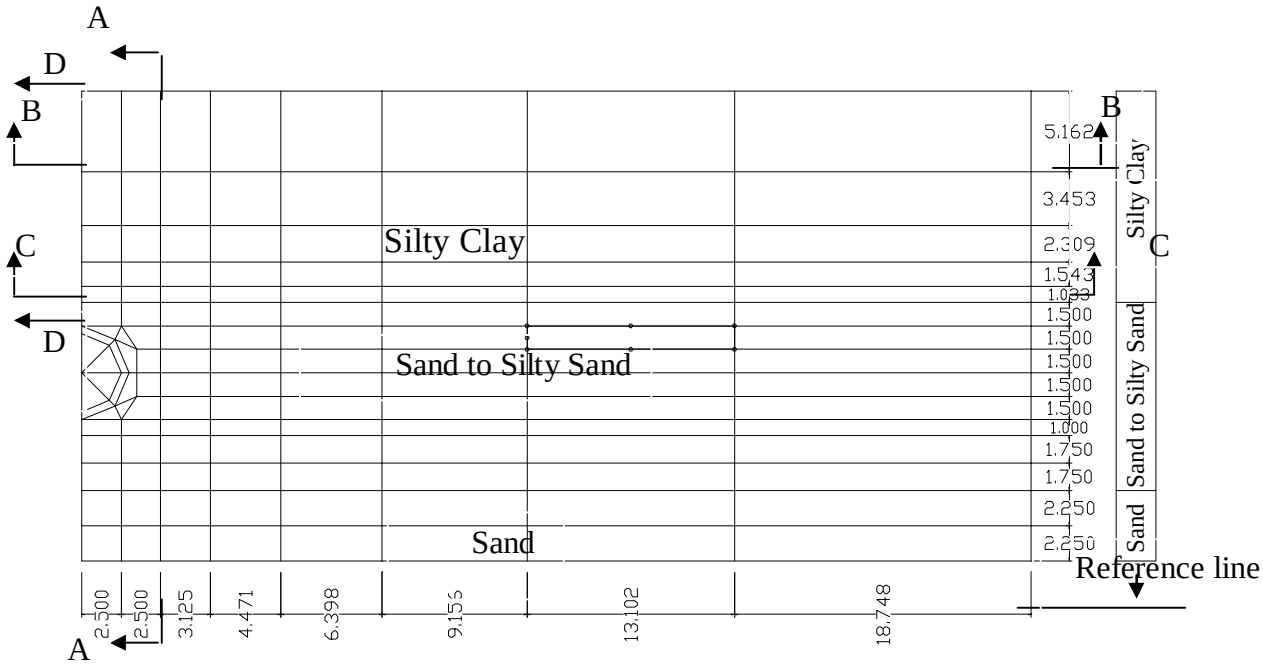

Figure (2) The finite element mesh for the basic problem.

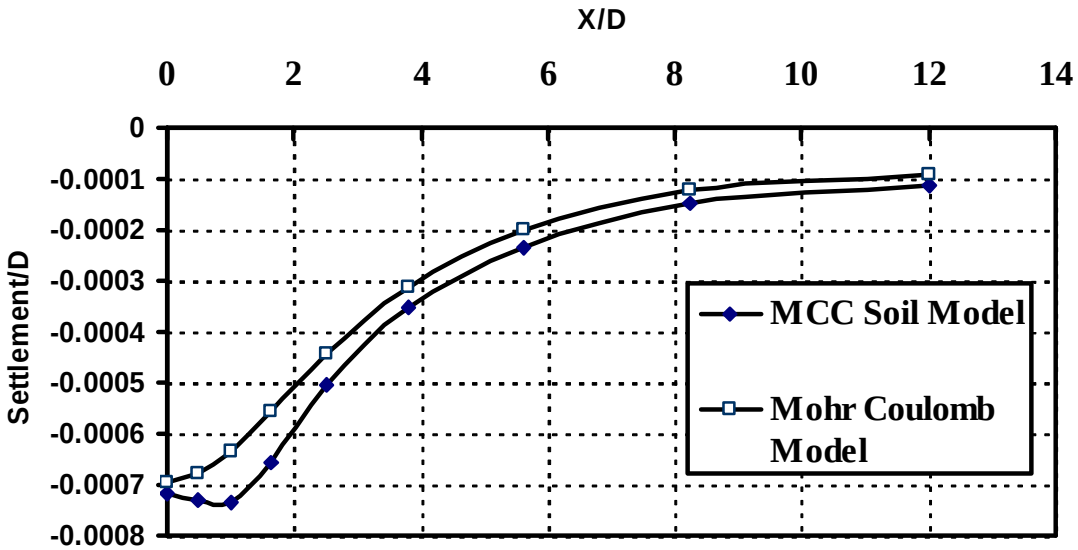

Figure (3) Soil surface subsidence using different soil models.

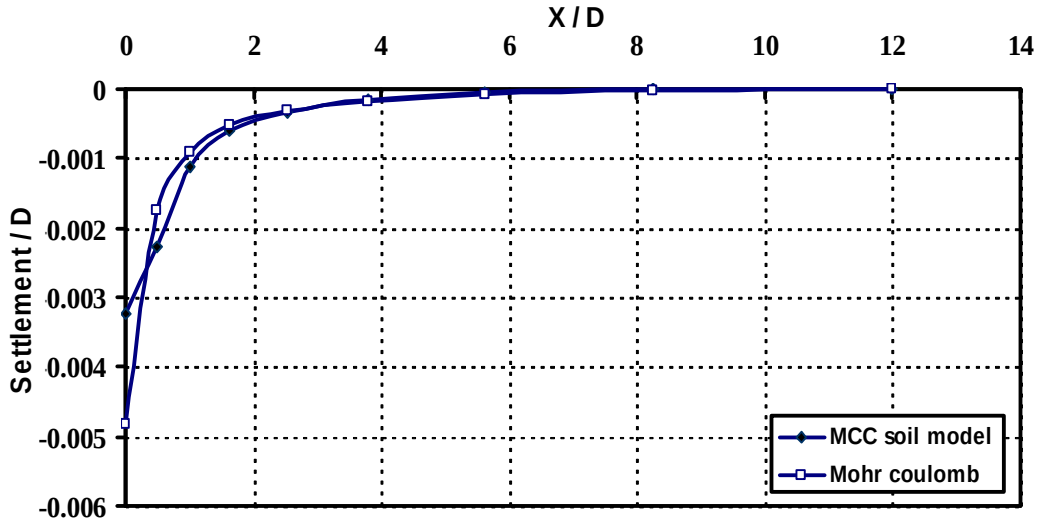

Figure (4) Comparison between settlements above the crown along section (C-C) using two soil models.

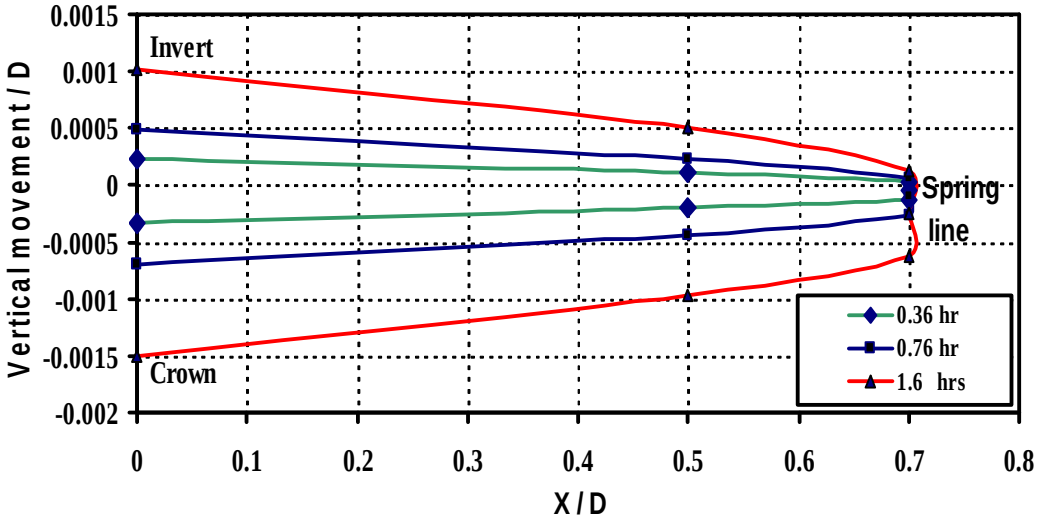

Figure (5): Vertical movement around the tunnel using Mohr-Coulomb failure criterion for the first layer

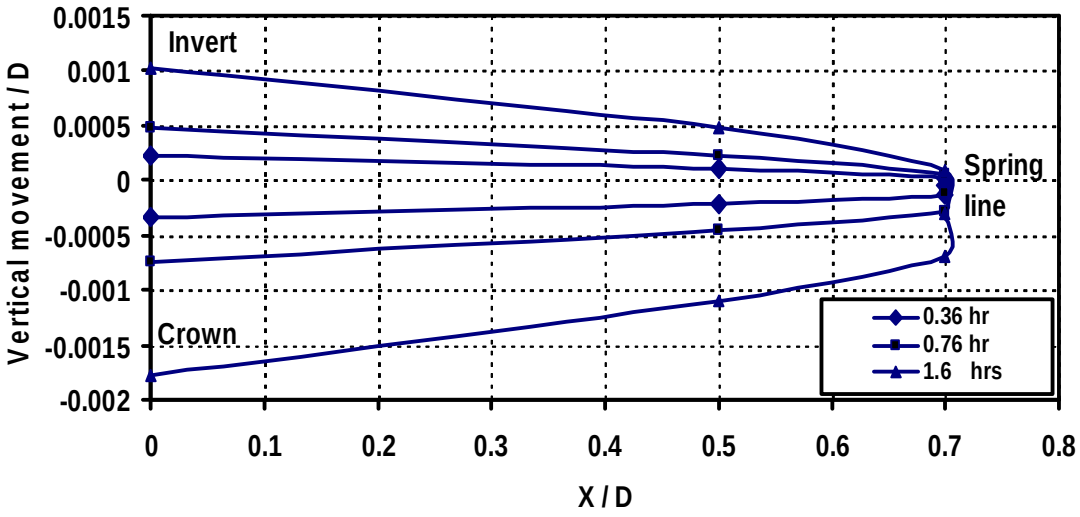

Figure (6): Vertical movement around the tunnel using MCC model for the first layer.

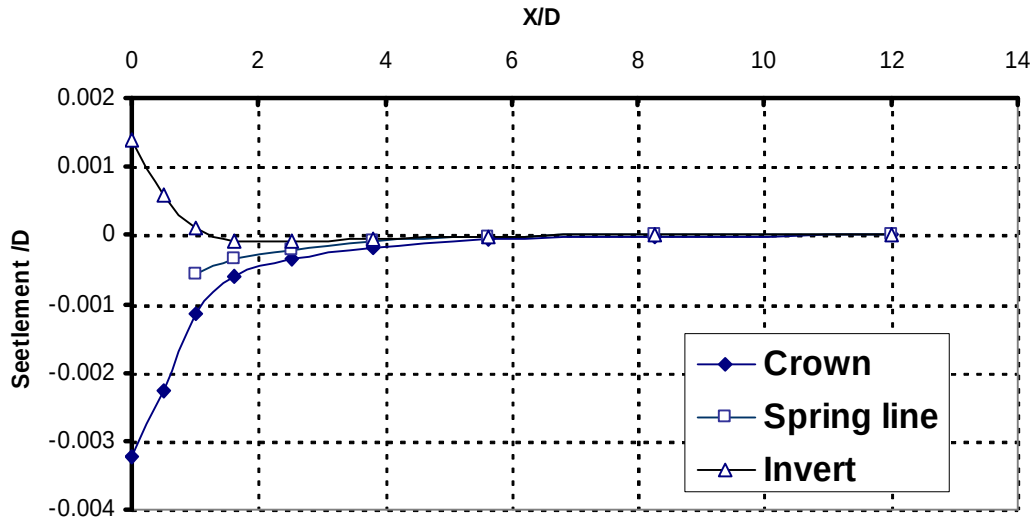

Figure (7): Vertical displacement at the end of excavation of the tunnel using MCC model.

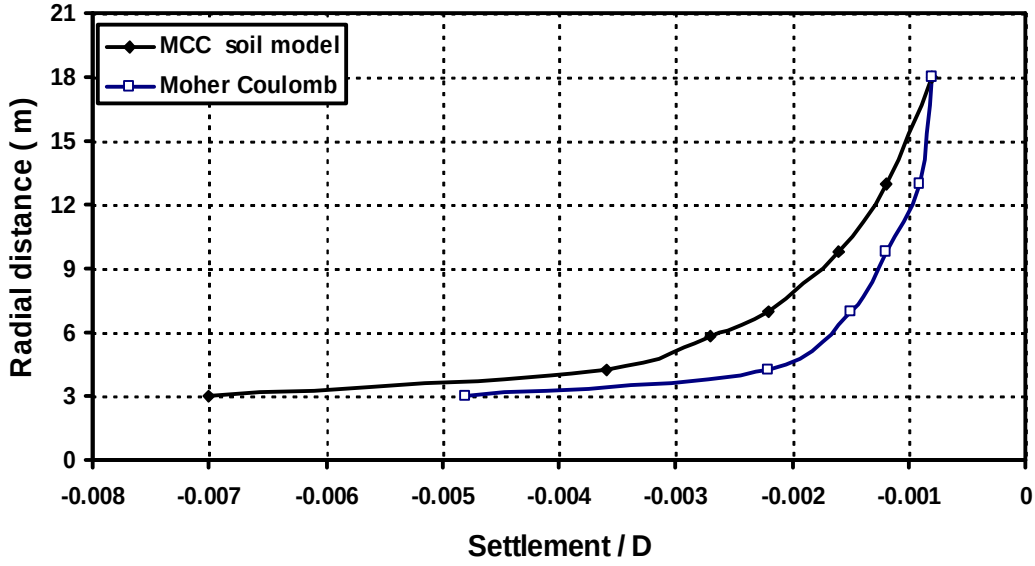

Figure (8): Variation of the vertical settlement along the radial distance of section D-D above the crown.

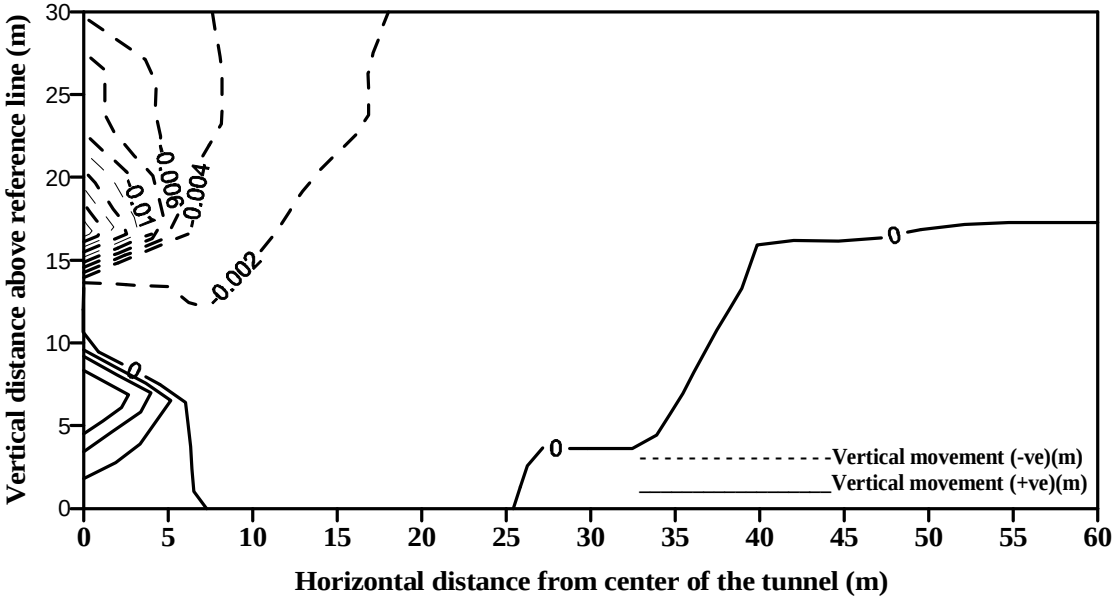

Figure (9): Contour lines of vertical movement (m).

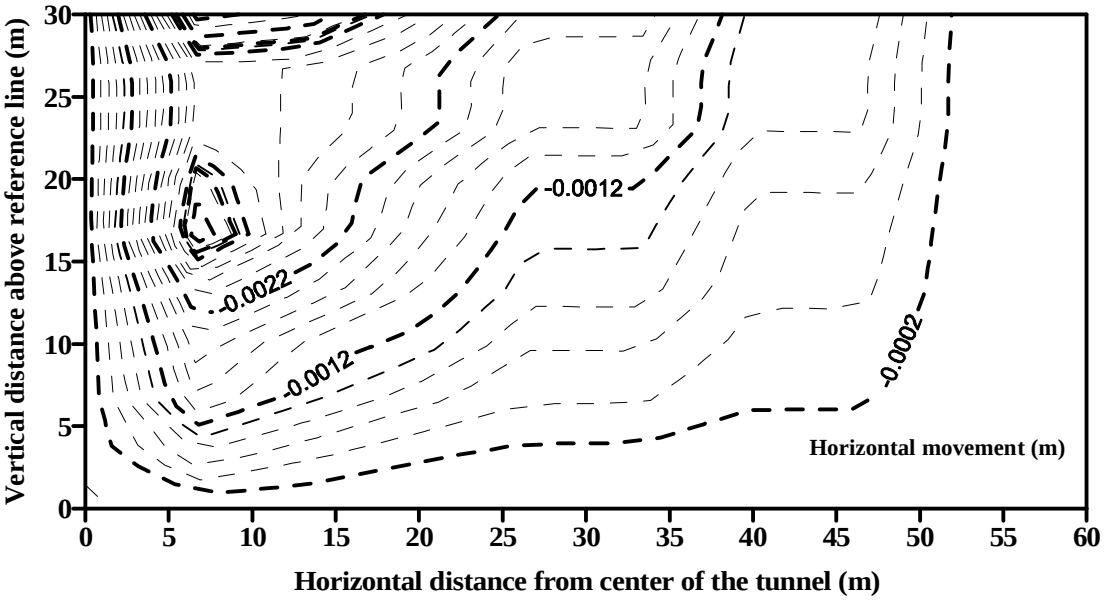

Figure (10): Contour lines of horizontal movement (m).

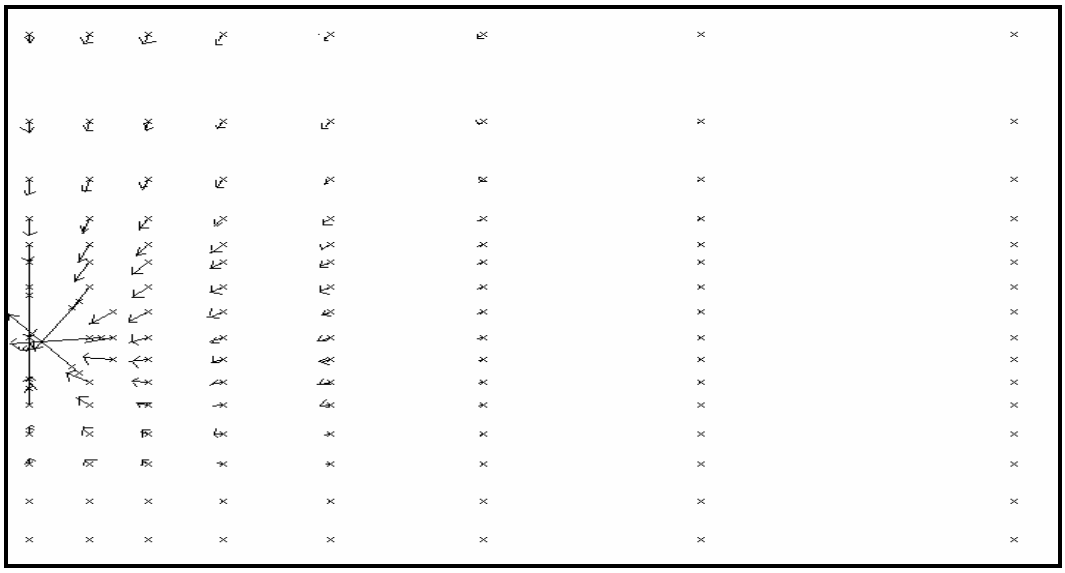

Figure (11): Displacement vectors around the tunnel for the basic problem (magnification factor = 150).

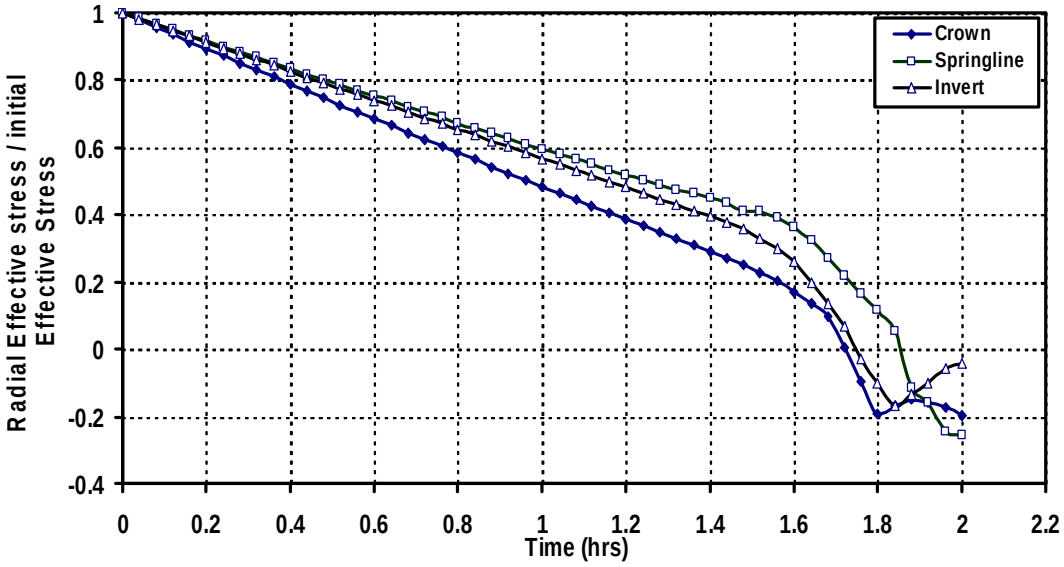

a- Radial stresses

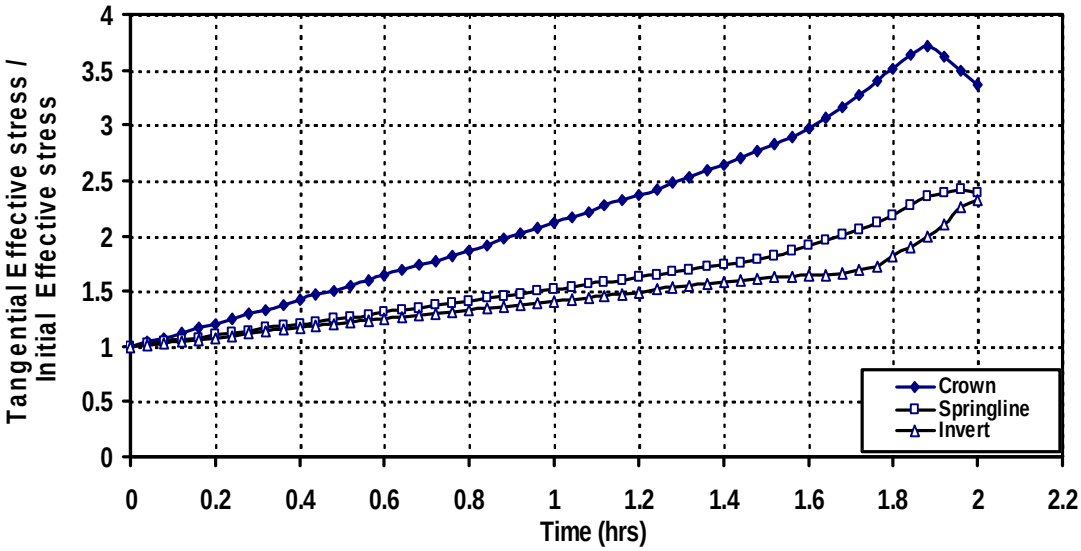

b- Tangential stresses.

Figure (12): Variation of stresses around the tunnel at the end of excavation.

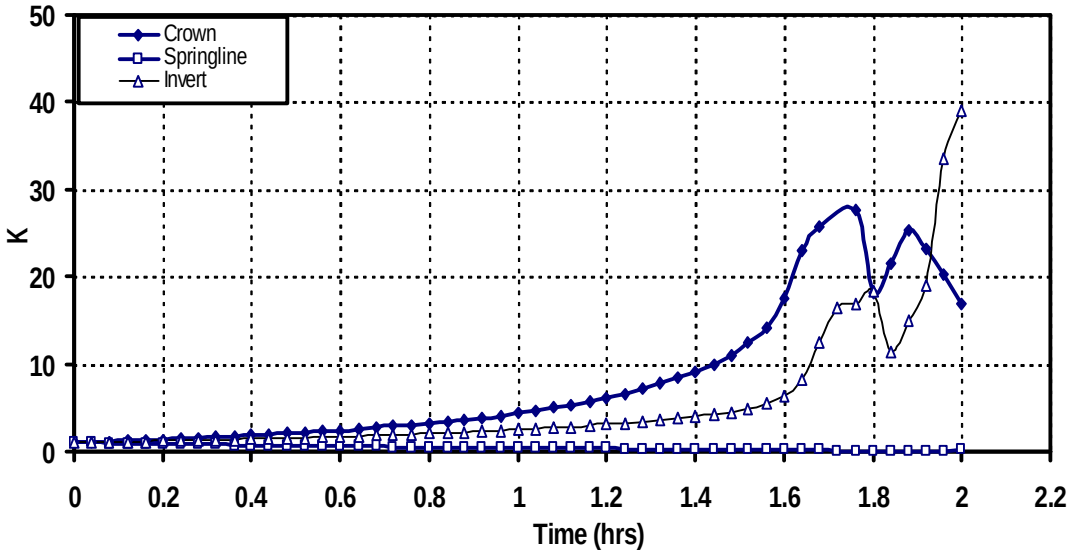

Figure (13): The variation of K at the crown, spring line and invert during the excavation of the tunnel.

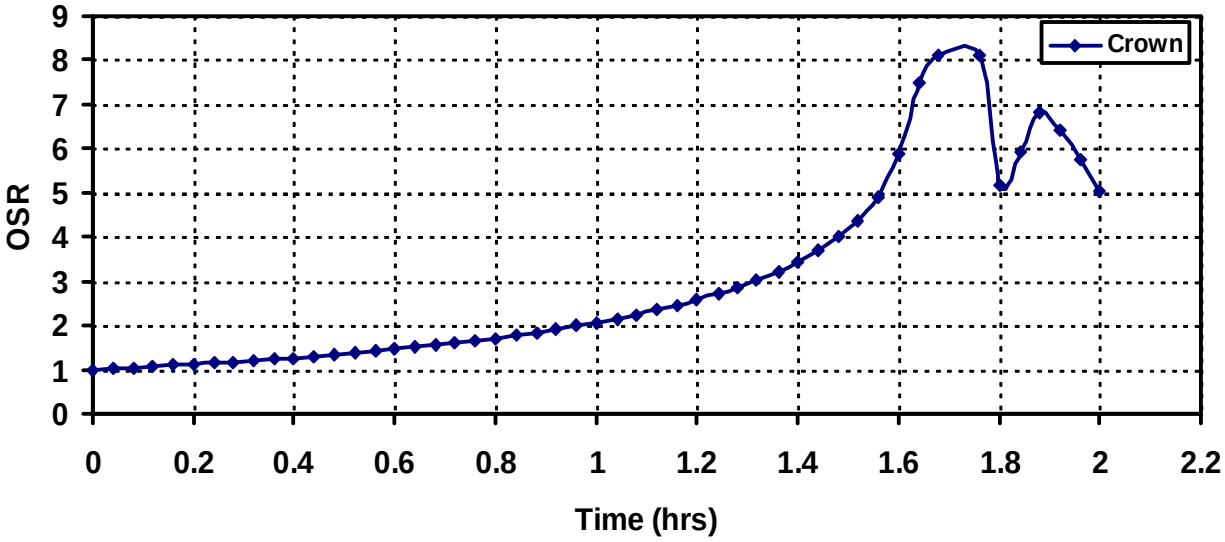

Figure (14): Variation of the overstress ratio (OSR) with time above the tunnel's crown.

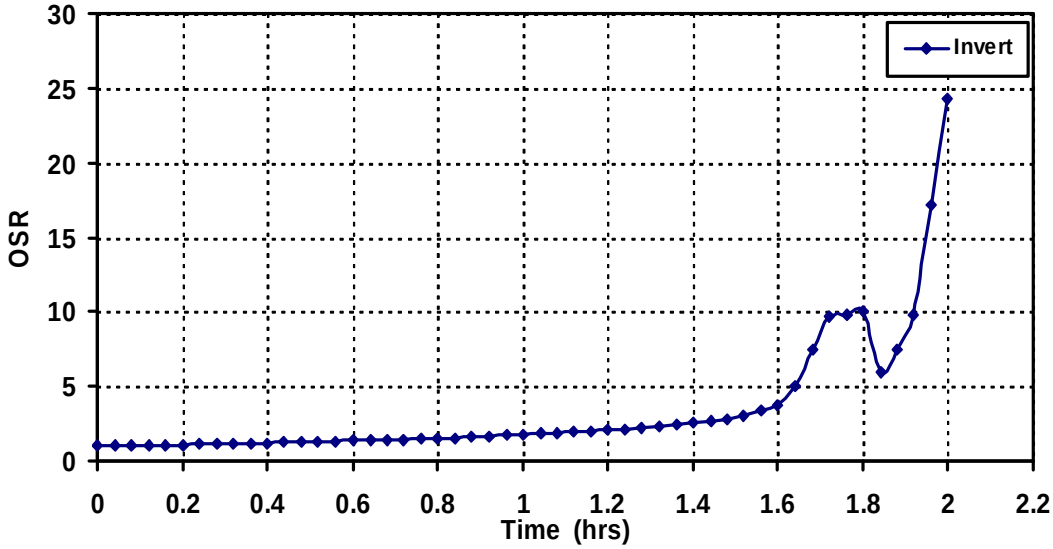

Figure (15): Variation of the over stress ratio (OSR) below the tunnel's invert.

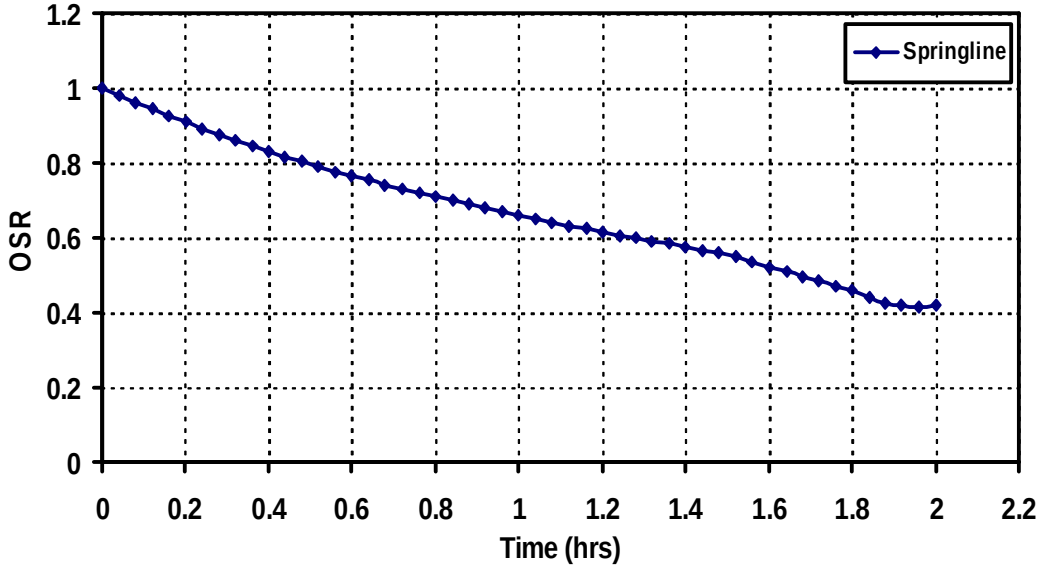

Figure (16): Variation of the over stress ratio OSR at the tunnel's spring line.

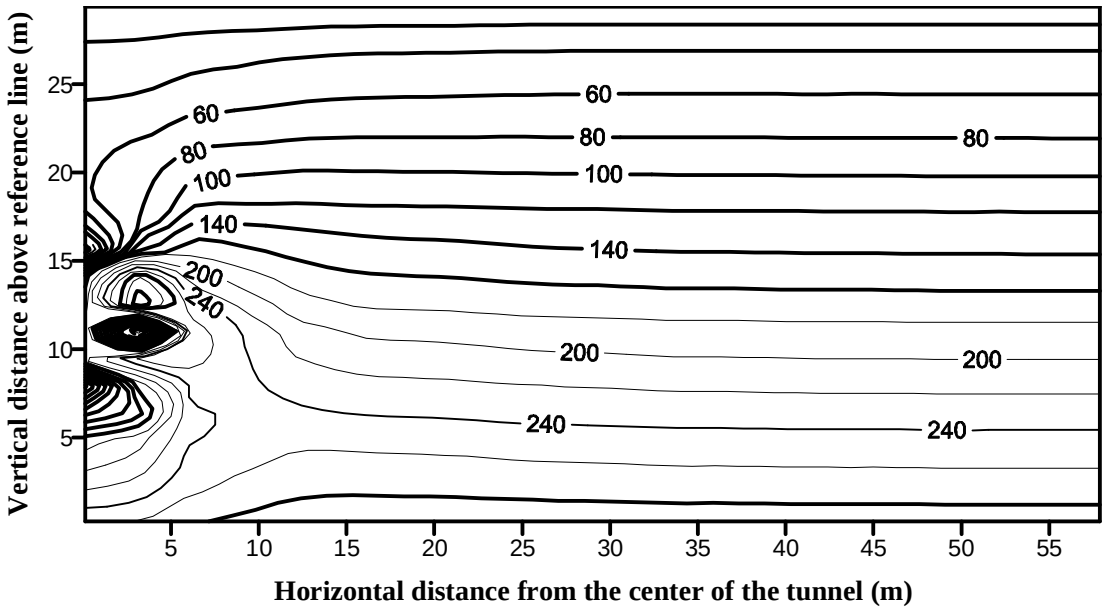

Figure (17): Contour lines of effective vertical stress in (kPa) at the end of excavation.

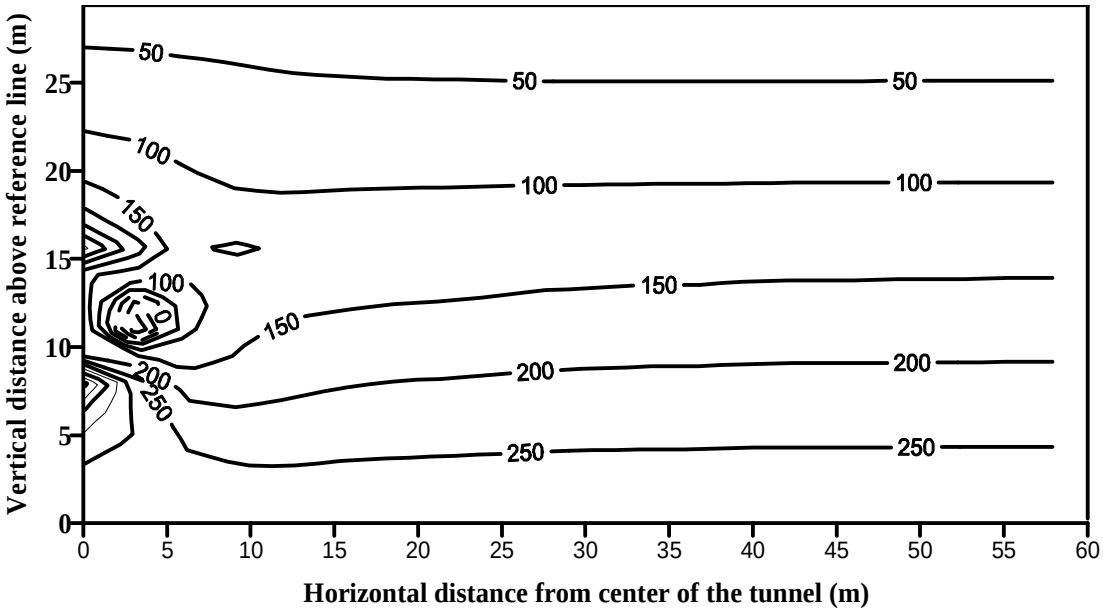

Figure (18): Contour lines of effective horizontal stress in (kPa) at the end of excavation.

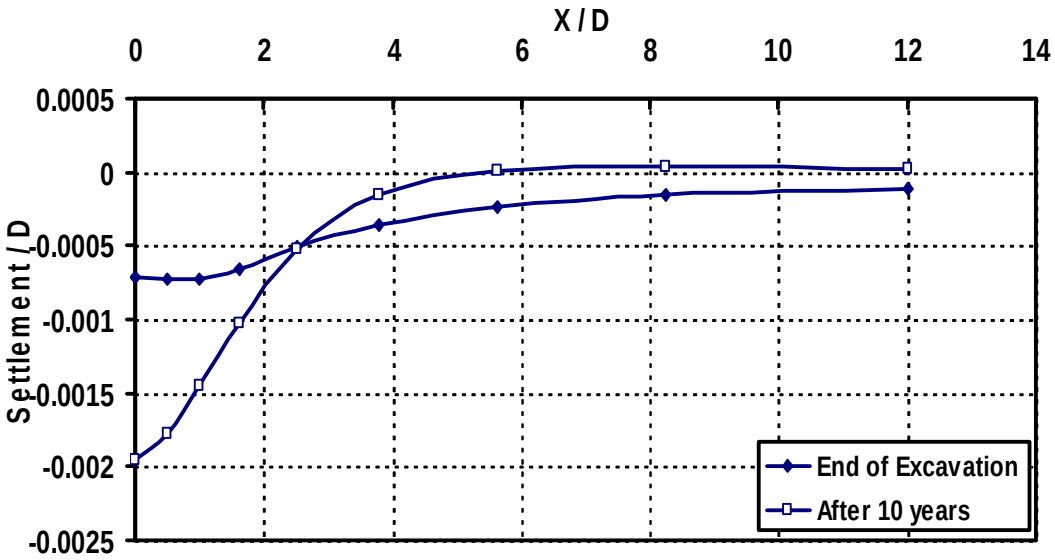

Figure (19): The surface settlement at the end of excavation and after consolidation using MCC soil model.

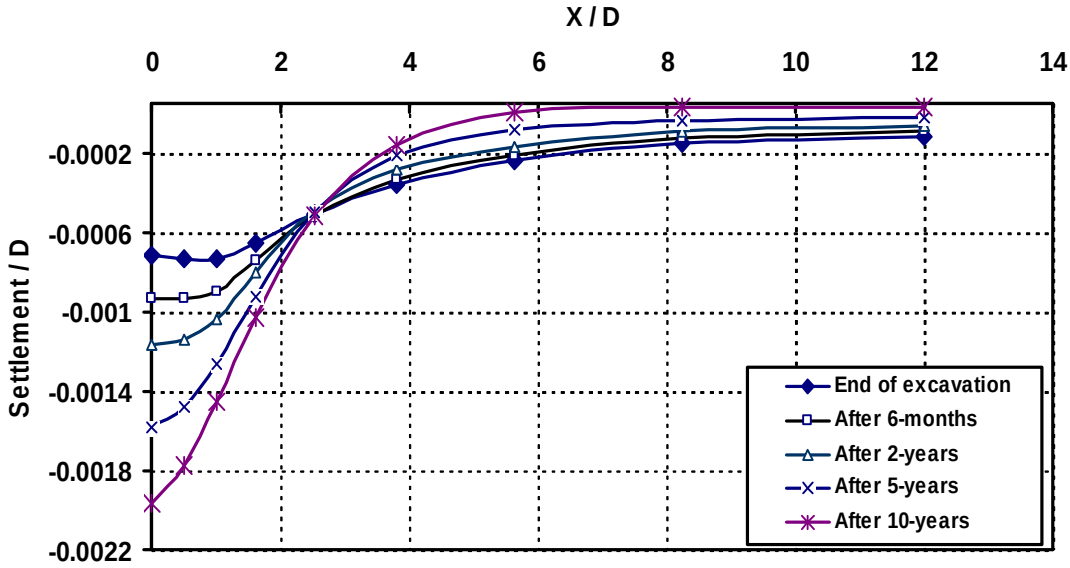

Figure (20): The surface settlement at different times using MCC soil model.

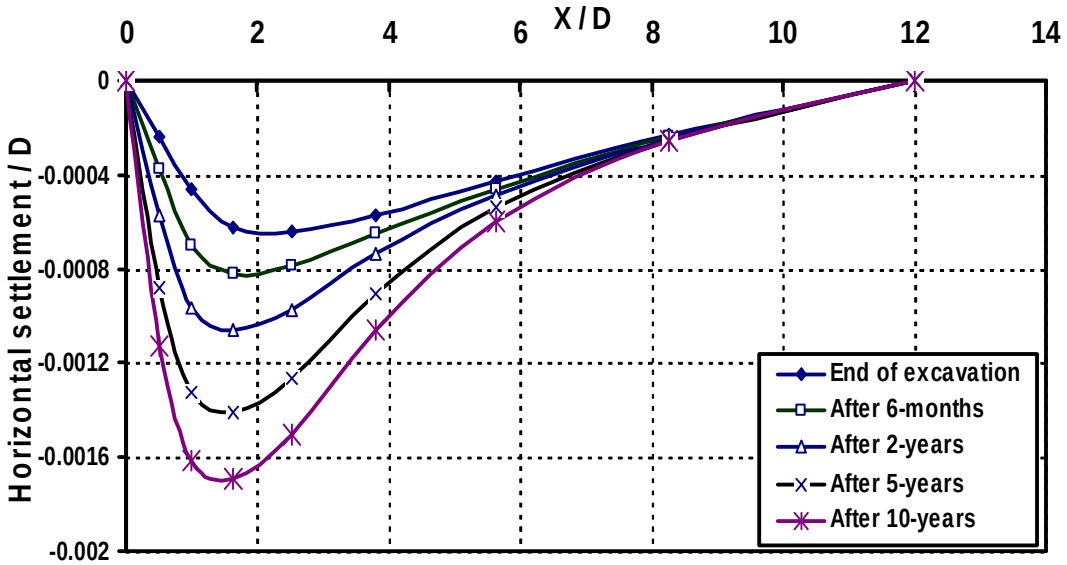

Figure (21): Surface horizontal displacement at the end of excavation and different times consolidation using MCC soil model

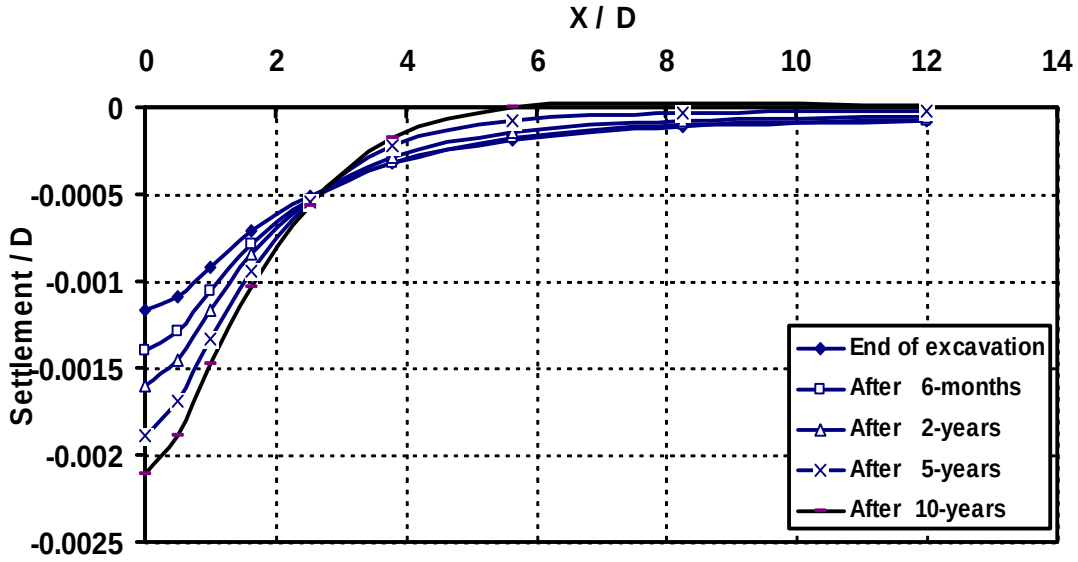

Figure (22): The variation of subsurface settlement along section B-B at different consolidation times using MCC soil model.

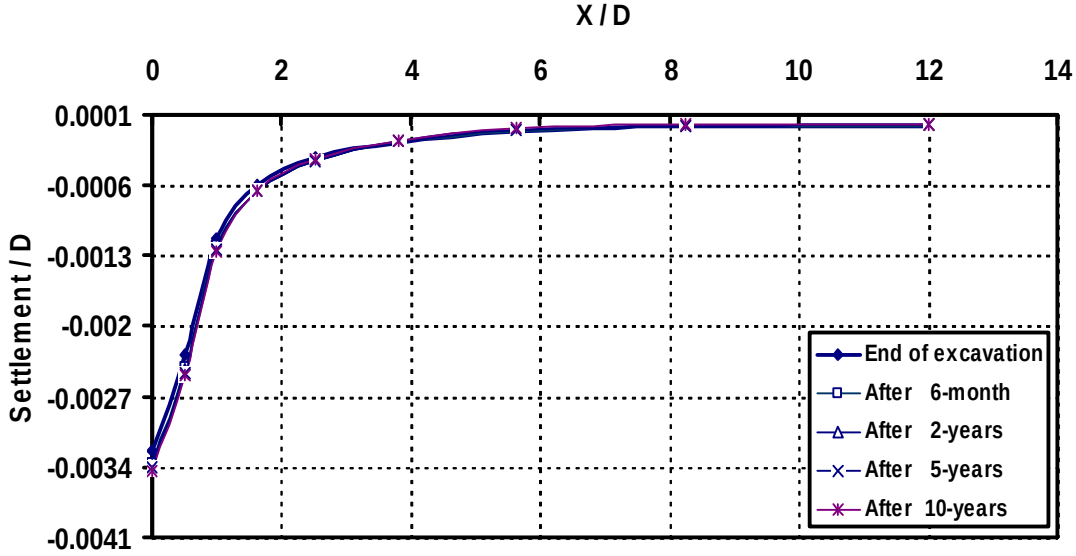

Figure (23): Subsurface settlement along section C-C at different consolidation times using MCC soil model.

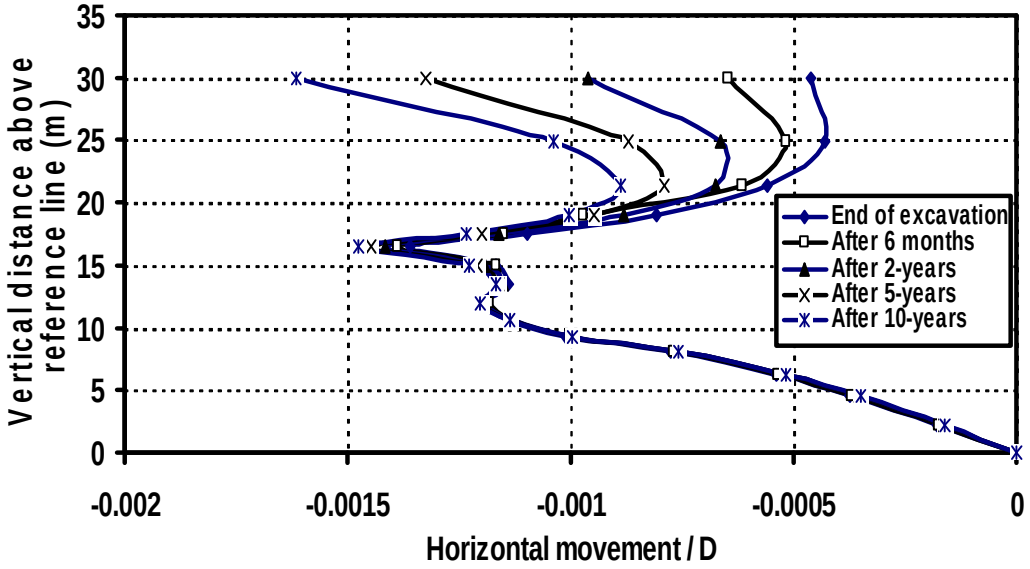

Figure (24): Vertical profile of horizontal displacement along section A-A during construction and consolidation stages using MCC soil model.

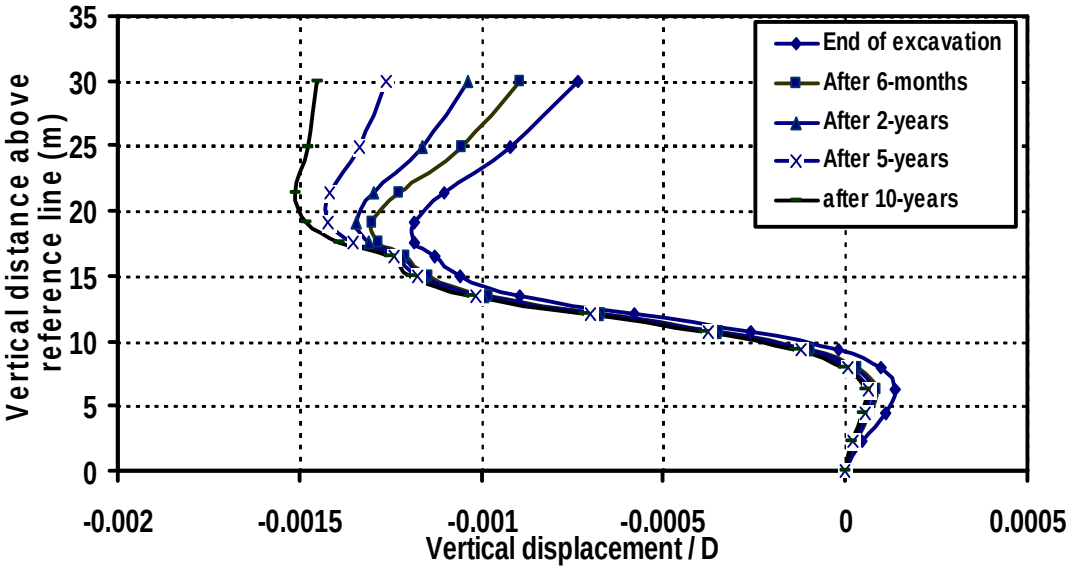

Figure (25): Variation of vertical displacement along section A-A during construction and consolidation stages using MCC soil model.